

Mott-Hubbard exciton in the optical conductivity of YTiO_3 and SmTiO_3

A. Gössling,¹ R. Schmitz,² H. Roth,¹ M. W. Haverkort,¹ T. Lorenz,¹ J. A. Mydosh,¹
E. Müller-Hartmann,² and M. Grüninger^{1,3}

¹*II. Physikalisches Institut, Universität zu Köln, Zùlpicher Strasse 77, D-50937 Köln, Germany*

²*Institut für Theoretische Physik, Universität zu Köln, Zùlpicher Strasse 77, D-50937 Köln, Germany*

³*2. Physikalisches Institut A, RWTH Aachen University, Otto-Blumenthal-Strasse, D-52074 Aachen, Germany*

(Received 16 May 2008; published 26 August 2008)

In the Mott-Hubbard insulators YTiO_3 and SmTiO_3 we study optical excitations from the lower to the upper Hubbard band, $|d^1 d^1\rangle \rightarrow |d^0 d^2\rangle$. The multipeak structure observed in the optical conductivity reflects the multiplet structure of the upper Hubbard band in a multiorbital system. Absorption bands at 2.55 and 4.15 eV in the ferromagnet YTiO_3 correspond to final states with a triplet d^2 configuration, whereas a peak at 3.7 eV in the antiferromagnet SmTiO_3 is attributed to a singlet d^2 final state. A strongly temperature-dependent peak at 1.95 eV in YTiO_3 and 1.8 eV in SmTiO_3 is interpreted in terms of a Hubbard exciton, i.e., a charge-neutral (quasi-) bound state of a hole in the lower Hubbard band and a double occupancy in the upper one. The binding to such a Hubbard exciton may arise both due to Coulomb attraction between nearest-neighbor sites and due to a lowering of the kinetic energy in a system with magnetic and/or orbital correlations. Furthermore, we observe anomalies of the spectral weight in the vicinity of the magnetic ordering transitions, both in YTiO_3 and SmTiO_3 . In the G -type antiferromagnet SmTiO_3 , the *sign* of the change of the spectral weight at T_N depends on the polarization. This demonstrates that the temperature dependence of the spectral weight is not dominated by the spin-spin correlations, but rather reflects small changes of the orbital occupation.

DOI: [10.1103/PhysRevB.78.075122](https://doi.org/10.1103/PhysRevB.78.075122)

PACS number(s): 71.20.Be, 71.27.+a, 77.84.Dy, 78.20.-e

I. INTRODUCTION

In strongly correlated electron systems, the competition between kinetic energy and Coulomb repulsion gives rise to a variety of intriguing phenomena.^{1,2} The most simple approach is the single-band Hubbard model, with on-site Coulomb repulsion U and a kinetic part proportional to the inter-site hopping amplitude t . For U larger than the bandwidth, the band splits into a lower and an upper Hubbard band (LHB and UHB; see inset of Fig. 1). At half filling one finds a Mott-Hubbard insulator with one localized electron per site, i.e., the Coulomb energy dominates. However, the low-energy physics is determined by the kinetic energy: Virtual hopping of the electrons to neighboring sites is effectively described by exchange interactions with $J \propto t^2/U$. These govern the spin degrees of freedom and, in a multiorbital model, are also relevant for the orbital degrees of freedom.³⁻⁵

The competition between Coulomb energy and kinetic energy also governs the formation of bound states, e.g., excitons. In simple band insulators, binding of an electron in the conduction band and a hole in the valence band reduces the Coulomb energy, while the kinetic energy increases. In Mott-Hubbard insulators, the lowest optical “interband” excitation creates an empty site and a doubly occupied site, i.e., a hole in the LHB and a particle in the UHB. A Hubbard exciton can be regarded as a bound state of an empty site and a doubly occupied site, moving in a background of singly occupied sites. Studies of excitons in correlated electron systems thus far have focused on one-(1D) or two-dimensional (2D) systems. Remarkably, it has been found that exciton binding can be driven by either the Coulomb energy or the kinetic energy. The former is found in the 1D extended Hubbard model, which takes into account the Coulomb interaction V between nearest or next-nearest-neighbor sites.⁶⁻¹⁴ Since *both* the Mott-Hubbard gap and the attractive interac-

tion for exciton binding result from Coulomb interactions, one expects different physics compared to band insulators. In fact, excitons are only formed below the gap if V exceeds a critical value.^{6,7,9,11} For smaller values of V , an excitonic resonance is found in the continuum above the gap, strongly affecting the line shape of the optical conductivity $\sigma(\omega)$.^{9,11,14} An exciton below the gap has been observed in 1D Ni-halogen chains,^{15,16} and this exciton contributes to the gigantic nonlinear optical response observed in these compounds.¹⁴⁻¹⁷

The kinetic energy is of prime importance for excitons in the 2D cuprates,¹⁸⁻²⁹ which are of charge-transfer type. The dispersion of a spinless charge-transfer exciton is of order t , *larger* than the single-particle dispersion, which is suppressed to $\sim J$ by antiferromagnetic (AF) correlations. Thus exciton formation reduces the *kinetic* energy,¹⁸⁻²² which bears resemblance to a possible mechanism for Cooper pair formation in high- T_c superconductors.^{21,30,31} Experimentally,

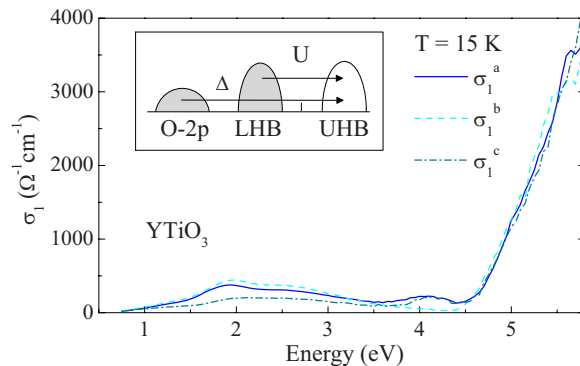


FIG. 1. (Color online) Optical conductivity of YTiO_3 at 15 K. Inset: sketch of the optical excitations from the LHB and the oxygen 2p band into the UHB in case of a single, half-filled orbital at the transition-metal site.

the exciton dispersion has been studied by electron-energy-loss spectroscopy¹⁹ and by resonant inelastic x-ray scattering (RIXS).^{28,29} It has been claimed that the dispersion is indeed large,^{19,28} but recent high-resolution RIXS data²⁹ indicate that the exciton dispersion is suppressed by the coupling to phonons.

Here, we report on the observation of an excitonic resonance in the optical conductivity $\sigma(\omega)$ of the three-dimensional (3D) Mott-Hubbard insulators YTiO₃ and SmTiO₃. The former is ferromagnetic below $T_c=27$ K, the latter is antiferromagnetic below $T_N=53$ K, and both exhibit orbital order.^{32–34} Due to the orbital multiplicity in these d^1 spin $S=1/2$ compounds, the upper Hubbard band consists of a series of different d^2 multiplets. In YTiO₃, the lowest multiplet is identified with a peak at 2.55 eV, whereas a strongly temperature-dependent peak at 1.95 eV is attributed to an excitonic resonance. For a proper determination of U it is essential to take excitonic effects into account. We discuss the possible relevance of the kinetic energy for exciton formation in *orbitally* ordered compounds, similar to the case of a 2D antiferromagnet. Our results provide the experimental basis to disentangle the role of Coulomb and kinetic energy in 3D Mott-Hubbard insulators.

The spectral weight of the LHB-UHB excitation is expected to depend on the nearest-neighbor spin-spin correlations.^{35–38} In a single-band model, the spectral weight vanishes in the case of ferromagnetic order due to the Pauli principle, and one expects a strong change of the spectral weight as a function of the temperature T at the magnetic ordering transition. In a multiorbital system, the spectral weight also depends on the orbital occupation. This kind of analysis has been applied to a number of compounds with different transition-metal ions (Mn, V, Ru, Mo).^{4,35–46} For instance in LaMnO₃ and LaSrMnO₄, a quantitative description of the experimentally observed T dependence of the spectral weight has been obtained.^{35,38} In the manganites, the T dependence is entirely ascribed to the spin-spin correlations, whereas the orbital occupation is assumed to be independent of T . This reflects the large ligand-field splitting Δ_{eg} of roughly 1 eV of the e_g orbitals in these d^4 compounds.^{35,38} Here, we show that the T dependence of the spectral weight of YTiO₃ and SmTiO₃ is *not* dominated by the spin-spin correlations. This is particularly evident for SmTiO₃, where the sign of the T dependence of the spectral weight depends on the polarization. This behavior can be attributed to small changes of the orbital occupation in these t_{2g} compounds.

The paper is organized as follows: Sec. II addresses the experimental details. The optical conductivity of YTiO₃ and SmTiO₃ is reported in Sec. III. In Sec. III A we first discuss the multiplet assignment and argue that the lowest peak has to be interpreted as an excitonic resonance in both compounds. A possible contribution of the kinetic energy to exciton binding in the case of antiferro-*orbital* order is proposed in Sec. III B. In Sec. III C we discuss the temperature dependence of the spectral weight and the relevance of spin-spin correlations and orbital occupation. The anisotropy of the spectral weight of the lowest multiplet in YTiO₃ is addressed in Sec. III D. A summary and conclusions are given in Sec. IV. The role of oxygen defects for the analysis of ellipsometric data of YTiO₃ is discussed in the Appendix.

II. EXPERIMENT

Single crystals of YTiO₃ and SmTiO₃ were grown using the floating-zone technique. The crystal quality and stoichiometry were checked by x-ray diffraction, energy dispersive x-ray (EDX), and polarization microscopy. The crystals are single phase and single domain. From magnetization measurements [superconducting quantum interference device (SQUID) magnetometer, vibrating sample magnetometer] we find that YTiO₃ becomes ferromagnetic below $T_c=27$ K and SmTiO₃ antiferromagnetic below $T_N=53$ K. Further details on crystal preparation and characterization can be found in Ref. 47. In YTiO₃, four-sublattice orbital order has been reported up to room temperature.^{32,33} In both compounds an orbital-ordering transition has not been observed, i.e., they are considered to be orbitally ordered up to the melting temperature, or, in other words, the distortions arising from the orbital occupation do not break the crystal symmetry.

Generalized ellipsometric data⁴⁸ was obtained using a rotating-analyzer ellipsometer (Woollam VASE) equipped with a retarder between polarizer and sample. The angle of incidence was 70°. Immediately after polishing, the sample was kept in an UHV cryostat. The measurement background pressure of $p < 10^{-9}$ mbar has been achieved by a bakeout at 400 K for 24 h. Window effects have been corrected using a standard Si wafer. In orthorhombic RTiO₃, only the diagonal elements σ^a , σ^b and σ^c of the complex optical conductivity tensor $\sigma(\omega)=\sigma_1+i\sigma_2$ are finite. In YTiO₃, we have determined $\sigma(\omega)$ from the normalized Müller matrix elements m_{12}^i , m_{21}^i , m_{33}^i , and m_{34}^i , where $i=1-4$ denotes different orientations of the sample, namely with s -polarized light parallel to the crystallographic a and b (a^* and c) axes on the ab (a^*c) surface, where $a^*=[110]$ within the $Pbnm$ space group. In SmTiO₃, $\sigma(\omega)$ has been determined from measurements on bc and ab surfaces.

Ellipsometry is a surface sensitive technique, thus one has to consider the possible contribution of surface contaminations or adsorbate layers. To this end we have polished and measured a sample of YTiO₃ several times, both in UHV and under ambient conditions, and for different angles of incidence. The raw data show small variations which are attrib-

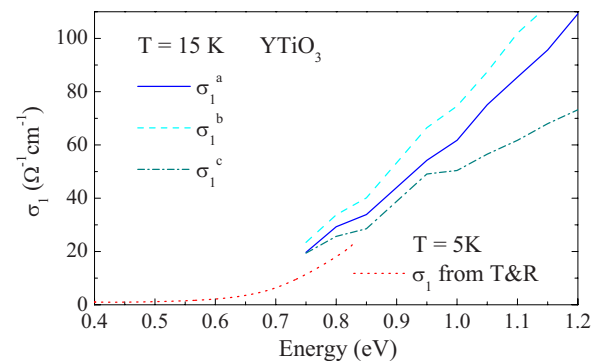


FIG. 2. (Color online) Optical conductivity of YTiO₃ in the vicinity of the onset of excitations across the gap. Good agreement is observed between our ellipsometry data and results determined from the combination of transmittance and reflectance measurements (Ref. 51).

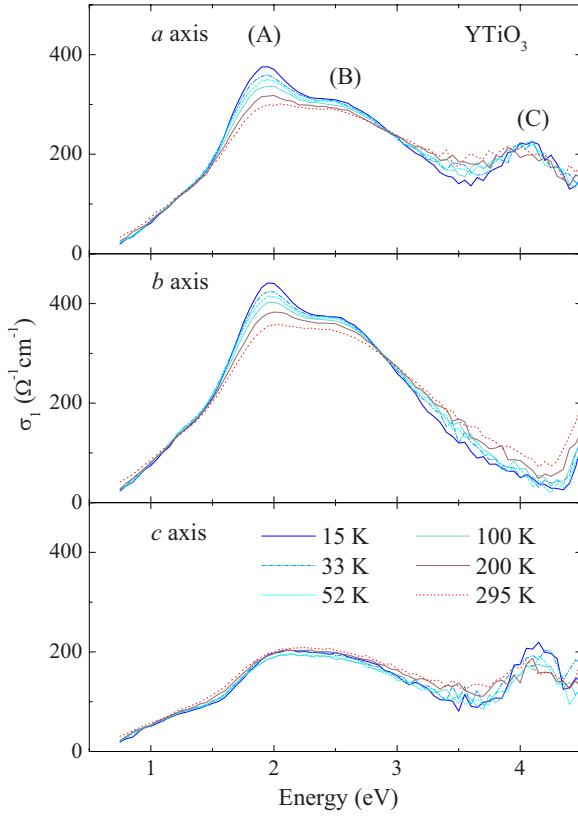


FIG. 3. (Color online) Optical conductivity of YTiO_3 below the onset of charge-transfer excitations, i.e., in the range of the lowest excitations from the lower to the upper Hubbard band. Peak B is attributed to the lowest multiplet, whereas peak A is identified as an excitonic resonance. Peak C reflects the lowest excitation to an e_g orbital.

uted to the surface. A consistent description of all data sets for the two distinct surface orientations has been achieved by assuming a nonabsorbing cover layer, where only the thickness $d \leq 2$ nm of this layer has been allowed to vary for different data sets. For an extensive discussion of the data analysis, we refer to Ref. 49. The particular choice of the cover layer has a certain influence on the absolute value of $\sigma(\omega)$, but we emphasize that the temperature dependence is hardly affected. We also have checked carefully that the observed temperature dependence reflects the properties of YTiO_3 and is not caused by changes of the cover layer, i.e., adsorbates.⁴⁹ We observed changes of the cover layer if we start with a base pressure of $p = 10^{-7}$ mbar, but not for $p < 10^{-9}$ mbar. In Fig. 1 we plot σ_1^a , σ_1^b , and σ_1^c of YTiO_3 from 0.75 to 5.8 eV at 15 K. The data are consistent with the unpolarized room-temperature data of Ref. 50 and with infrared transmittance and reflectivity results obtained in our group.⁵¹ The latter revealed an onset of interband excitations at about 0.6 eV (see Fig. 2). Recently, the effect of oxygen defects at the surface of YTiO_3 has been discussed.⁵² We address this issue in the Appendix.

III. RESULTS

Undoped YTiO_3 and SmTiO_3 are Mott-Hubbard insulators. In the ground state there is a single electron in the $3d$

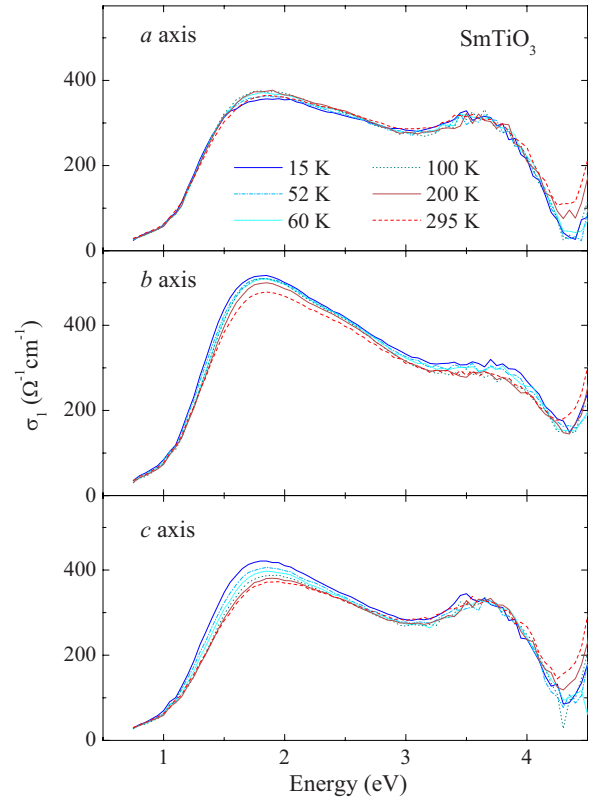


FIG. 4. (Color online) Optical conductivity of SmTiO_3 .

shell at each Ti site. It is well accepted that the absorption above the gap corresponds to excitations from the LHB to the UHB, i.e., to the creation of an empty and a doubly occupied site, $|d^1 d^1\rangle \rightarrow |d^0 d^2\rangle$. The strong increase of $\sigma_1(\omega)$ above ≈ 4.5 eV (see Fig. 1) reflects the onset of charge-transfer excitations from the O_{2p} band to the UHB, $|d^1 p^6\rangle \rightarrow |d^2 p^5\rangle$. The difference in spectral weight can be attributed to the Ti-O hopping t_{pd} : $\sigma_1(\omega) \propto t_{pd}^2$ for charge-transfer excitations and $\sigma_1(\omega) \propto t_{pd}^4 / \Delta^2$ for Mott-Hubbard excitations, where Δ denotes the charge-transfer energy.

For YTiO_3 , photoemission and inverse photoemission spectroscopy^{47,53-55} yield $\Delta \approx 6$ eV and an on-site Coulomb interaction $U \approx 5$ eV,⁵⁶ where U denotes the Coulomb repulsion if both electrons occupy the *same* real orbital. In a single-band Hubbard model, the splitting between LHB and UHB is given by U (cf. inset of Fig. 1). However, for a quantitative description of $\sigma(\omega)$ and for a reliable peak assignment one has to take all five $3d$ orbitals into account.³⁵⁻³⁸

A. Multiplet assignment and Hubbard exciton

Figures 3 and 4 focus on the inter-Hubbard-band excitations of YTiO_3 and SmTiO_3 below 4.5 eV. In YTiO_3 , three peaks are observed at 1.95 (A), 2.55 (B), and 4.15 eV (C). In SmTiO_3 , we find two pronounced peaks at 1.9 and 3.7 eV. Additionally, there is a shallow shoulder at 2.5 eV, particularly noticeable for the b axis.

For a Mott-Hubbard insulator, one expects that a local multiplet calculation yields a reasonable assignment of the LHB-UHB excitations.³⁵⁻³⁸ In terms of local multiplets, the

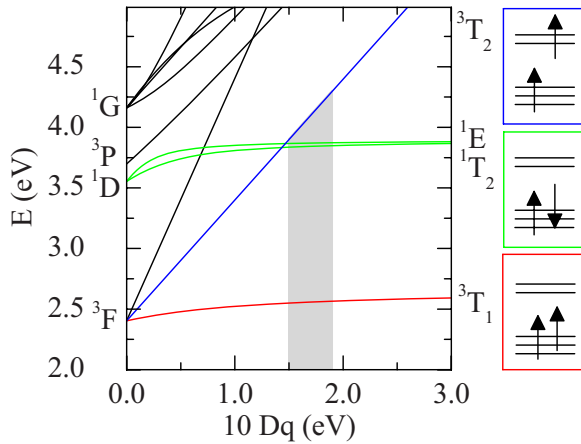


FIG. 5. (Color online) Left: Calculated energies for a $|d^1 d^1\rangle \rightarrow |d^0 d^2\rangle$ excitation with different d^2 final states in a cubic crystal field (Ref. 57). The Slater integrals were chosen as $F^0=3.60$ eV, $F^2=6.75$ eV, and $F^4=4.55$ eV, corresponding to $U=4.5$ eV (Ref. 56) and $J_H \approx 0.6$ eV. For $10Dq=0$ the ionic multiplet structure is obtained. For $10Dq \approx 1.5-1.9$ eV (gray area) the energy of 4.15 eV for peak C is well described by excitations into the 3T_2 state. Right: sketch of the orbital occupation in the strong crystal-field limit for the 3T_1 triplet (red), the 1T_2 and 1E singlets (green), and the 3T_2 triplet (blue).

excited $|d^0 d^2\rangle$ states can be distinguished according to the d^2 sector, because d^0 is an empty shell. The d^2 sector is split into a series of multiplets by the electron-electron interaction, the crystal field, and the hybridization with the ligands.⁵⁷ We start from cubic symmetry, in which case the crystal field and the hybridization give rise to a splitting of the $3d$ orbitals into a triply degenerate t_{2g} level and a doubly degenerate e_g level at higher energy. The splitting is denoted by $10 Dq$, which roughly can be estimated as 2 ± 0.5 eV.^{33,58-60} The electron-electron interaction within the $3d$ shell can be parameterized by the three Slater integrals F^0 , F^2 , and F^4 . Values of $F^2=6.75$ eV and $F^4/F^2 \approx 5/8$ are characteristic for d^2 Ti^{2+} ions in a crystal.⁵⁷ The only parameter that can be adapted is F^0 , which drastically deviates in a solid from the ionic value due to screening effects.

For $F^0=3.60$ eV [or $U \approx 4.5$ eV (Ref. 56)] the $|d^1 d^1\rangle \rightarrow |d^0 d^2\rangle$ excitation energies are given in Fig. 5, focusing on the four multiplets lowest in energy: the triplet 3T_1 , the singlets 1T_2 and 1E , and the triplet 3T_2 . For an intuitive picture we consider the strong crystal-field limit ($10 Dq \gg U$), as sketched on the right-hand side of Fig. 5. In this limit, there is one electron in the t_{2g} level and one in the e_g level in the 3T_2 state, whereas both electrons occupy the t_{2g} level in the three other states. It is common to consider the simplified Kanamori scheme³⁷ with the Hund on-site exchange coupling $J_H = \frac{2.5}{49} F^2 + \frac{22.5}{441} F^4$, resulting in $J_H = 0.6 \pm 0.1$ eV for d^2 Ti^{2+} . For $U \approx 4-5$ eV, the Kanamori scheme predicts the lowest excitation into the 3T_1 triplet at $U - 3J_H \approx 2-3$ eV, separated from the singlets 1T_2 and 1E by $2J_H \approx 1.2$ eV (reflecting Hund's rule) and from the 3T_2 state by $10 Dq \approx 2$ eV, in qualitative agreement with the result of the rigorous calculation shown in Fig. 5.

1. YTiO_3

Figure 5 clearly shows that the 3T_1 state is the lowest multiplet, more than 1.2 eV below the next multiplet for any reasonable choice of $10 Dq$. Thus the small splitting of 0.6 eV between peaks A and B in YTiO_3 cannot be identified with the difference between the 3T_1 state and any other multiplet. We conclude that both peaks A and B are related to excitations into the 3T_1 state. Peak C can be attributed to the 3T_2 state, since only excitations into triplet states are allowed from a fully polarized ferromagnetic ground state within an electric dipole approximation. Excitations to the singlet states 1T_2 and 1E require a spin flip and thus are suppressed, at least at low temperatures.

In the following, we discuss three scenarios for the splitting between peaks A and B: deviations from cubic symmetry, band-structure effects, and an excitonic resonance. The deviation from cubic symmetry lifts the degeneracy of the t_{2g} orbitals and thereby also of the 3T_1 state. The t_{2g} splitting was found to be ≈ 0.25 eV in infrared transmittance,⁵¹ Raman scattering,⁶¹ and RIXS measurements.⁵⁹ This is clearly too small to explain the splitting between peaks A and B.⁶²

Now we address the possible role of band-structure effects. Based on the actual crystal structure, a LDA+DMFT study of YTiO_3 by Pavarini *et al.*⁶³ does not show a splitting of the lowest peak in $\sigma_1(\omega)$. For $U=5$ eV and $J_H=0.64$ eV, this peak has been predicted at 3.3 eV, and the optical gap is expected roughly at 1.5 eV. This large value of the gap suggests that a smaller value of U is more appropriate. Good agreement between the prediction for the lowest peak and the observed energy of 2.55 eV of peak B can be obtained by assuming $U \approx 4.3$ eV. This value of U also yields a good description of the optical gap. Moreover, it corroborates the validity of our local multiplet calculation discussed above (see Fig. 5), which for $U=4.5$ eV predicts the lowest peak at about 2.5 eV. We stress that it is unreasonable to identify peak A at 1.95 eV with the peak found in LDA+DMFT, since this would require to assume a still smaller value of U , resulting in a very small gap. Indeed the LDA+DMFT calculation finds a metallic state for $U=3.5$ eV.⁶³

Also the LDA+DMFT study by Craco *et al.*⁶⁴ for the ferromagnetic phase of YTiO_3 finds a single peak in $\sigma_1(\omega)$. Based on the parameter values of $U=4.75$ eV and $J_H=1.0$ eV, Craco *et al.* attribute this peak to peak A observed at 1.95 eV in our data. However, J_H is not expected to deviate strongly from the ionic value of $J_H=0.6 \pm 0.1$ eV discussed above. The lowest peak in $\sigma_1(\omega)$ is located at about $U - 3J_H$, thus the choice of $J_H=1.0$ eV strongly underestimates the peak frequency. We emphasize that both LDA+DMFT studies^{63,64} find a *single* peak in $\sigma_1(\omega)$. Both studies investigate an effective Hamiltonian for the t_{2g} sector, i.e., excitations to the higher-lying 3T_2 multiplet (peak C) are not considered.

Experimental data also do not support a splitting due to band-structure effects. In photoemission (PES) data of YTiO_3 the LHB is a single peak ≈ 1.3 eV below the Fermi level.^{47,53,55,65} In inverse PES on $\text{Y}_{1-x}\text{Ca}_x\text{TiO}_3$ [$x=0$ (Ref. 65) and $0.4-0.8$ (Ref. 55)] the UHB can be identified with the lowest peak or shoulder $\approx 1.5-2$ eV above the Fermi

level. Both PES and inverse PES agree with the LDA+DMFT result⁶³ for $U=4-5$ eV. Finally, $U\approx 5.3$ eV has been derived from $2p$ core-level PES (Ref. 54) (see Ref. 56 for the comparison of parameters derived by different methods).

Altogether, both theoretical and experimental results support our interpretation that the splitting of 0.6 eV between peaks A and B does not result from the band structure and that peak B at 2.55 eV is the dominant excitation.

In contrast to (inverse) PES, the optical conductivity reflects particle-hole excitations and thus is sensitive to interactions between the particle in the UHB (i.e., a double occupancy) and the hole in the LHB. These interactions are also neglected in the LDA+DMFT calculations^{63,64} of $\sigma_1(\omega)$. We therefore identify peak B at 2.55 eV as a particle-hole excitation in which the particle and the hole are well separated, whereas peak A at 1.95 eV is interpreted as an excitonic resonance, where the particle and the hole remain close to each other. Note that peak A does not lie below the gap, i.e., it is not a truly bound exciton, but a resonance within the continuum. As discussed above, a Hubbard exciton may arise due to the attractive Coulomb interaction between the particle and the hole. The nearest-neighbor electron-electron repulsion V of the extended Hubbard model⁶⁻¹⁴ is equivalent to a particle-hole attraction $-V$.⁶⁶ We are not aware of an accurate experimental value of V for the titanates, but it is reasonable to assume $V\leq 1$ eV. For the 1D charge-transfer insulator SrCuO₂, a value of $V\approx 0.6$ eV has been derived from the comparison of the line shape of the excitonic resonance in $\sigma_1(\omega)$ with predictions from dynamical density-matrix renormalization group calculations for an effective extended Hubbard model.¹³ More detailed theoretical studies of the extended Hubbard model in 3D are required to decide whether the nearest-neighbor Coulomb interaction is sufficient to explain the splitting of 0.6 eV observed between peaks A and B. A possible contribution of the kinetic energy to the attractive interaction is discussed below in Sec. III B.

In the context of an exciton interpretation of the lowest peak at 1.95 eV, one also has to consider the possibility of a charge-transfer exciton. However, the lowest Mott-Hubbard excitation is expected at $U-3J_H\approx 2-3$ eV, which is much smaller than the charge-transfer energy $\Delta\approx 6$ eV. The observed onset of charge-transfer excitations at 4.5 eV shows that an explanation of the peak at 1.95 eV in terms of a charge-transfer exciton requires a binding energy of more than 2.5 eV, which we consider to be very unlikely. Moreover, the relative spectral weight of a bound state in general increases with increasing binding energy. For instance the calculation of the Mott-Hubbard exciton in 1D shows that the spectral weight is transferred almost entirely to the exciton as soon as a true bound state is formed,¹¹ hardly any weight remains within the continuum. In RTiO₃, the spectral weight of the charge-transfer excitations is much larger than the weight of the Mott-Hubbard excitations, and we expect that a truly bound charge-transfer exciton with a binding energy as large as 2.5 eV should show a larger spectral weight than observed.

2. SmTiO₃

The magnetic ground state of RTiO₃ changes from ferromagnetic to antiferromagnetic as a function of the size of the

R ions.^{67,68} This change is accompanied by a crossover for both the character of the distortions of the oxygen octahedra and of the orbital-ordering pattern.^{34,67-69} The optical conductivity of the antiferromagnet SmTiO₃ is given in Fig. 4, focusing on the range of the Mott-Hubbard bands below the onset of charge-transfer excitations at about 4.5 eV. At 300 K we observe two pronounced peaks at 1.9 and 3.7 eV and a shallow shoulder at 2.5 eV, most evident for the b axis. The multiplet structure discussed above for YTiO₃ also applies to SmTiO₃. In particular, one does not expect appreciable changes of the Slater integrals, i.e., of the electronic parameters U and J_H . This is corroborated by the LDA+DMFT calculations by Pavarini *et al.*,⁶³ which predict the same peak frequency for $\sigma_1(\omega)$ in YTiO₃ and in the antiferromagnet LaTiO₃. Therefore we identify the shoulder at 2.5 eV in SmTiO₃ with peak B at 2.55 eV in YTiO₃, whereas the asymmetric peak at 1.8 eV is attributed to an excitonic resonance (see below), equivalent to peak A in YTiO₃.

In contrast to the peak energies, the bandwidth or equivalently the hopping matrix elements are expected to change significantly, resulting from the different Ti-O-Ti bond angles. A larger bandwidth of SmTiO₃ agrees with the observation from transmittance measurements⁵¹ that the gap in SmTiO₃ is about 0.2 eV lower than in YTiO₃. Additionally, an increase of the hopping amplitudes gives rise to an increase of the spectral weight. This is further enhanced by the change of the orbital ground state.^{67,68} Experimentally, we find an increase of N_{eff} [cf. Eq. (1)] from YTiO₃ to SmTiO₃ of roughly 25%, 50%, and 100% for the a , b , and c axes, respectively.

As discussed above for YTiO₃, an interpretation of the peak at 1.8 eV in terms of the lowest multiplet is hard to reconcile with the LDA+DMFT result,⁶³ unless excitonic effects are considered. An exciton interpretation is supported by the temperature dependence of the peak frequency observed for the b and c axes, showing an anomalous softening with decreasing temperature and an anomaly at T_N . For the b axis we demonstrate this softening in Fig. 6. We focus on the frequency ω_e of the leading edge, which we define as $\sigma_1^b(\omega_e)=350(\Omega\text{ cm})^{-1}$. This has the advantage that ω_e and also its temperature dependence can be determined more accurately than the peak frequency itself. The disadvantage is that a softening of ω_e in principle can be caused not only by a softening of the peak frequency, but also by an increase of either the spectral weight or the line width, and by a change of the line shape. We find a jumplike decrease of ω_e at T_N ; see lower panel of Fig. 6. This cannot be attributed to an increased linewidth, since the thermal contribution to the linewidth is expected to decrease with decreasing temperature. Moreover, for *spin-carrying* particles one expects that the bandwidth is reduced upon entering the AF ordered state, thus the gap is expected to *harden*. For an estimate of the T dependence of the spectral weight we consider the value of $\sigma_1(\omega)$ at the peak frequency. We find an increase of $\sigma_1^b(\omega=1.85\text{ eV})$ upon cooling below T_N (see crosses in bottom panel of Fig. 6), indicating an increase of the spectral weight. We use this T dependence of the absolute value to determine a corrected frequency of the leading edge, $\tilde{\omega}_e$, defined as $\sigma_1^b(\tilde{\omega}_e)=c\cdot 350(\Omega\text{ cm})^{-1}$ with $c=\sigma_1^b(1.85\text{ eV}, T)/\sigma_1^b(1.85\text{ eV}, 60\text{ K})$ (open symbols in Fig. 6). This shows

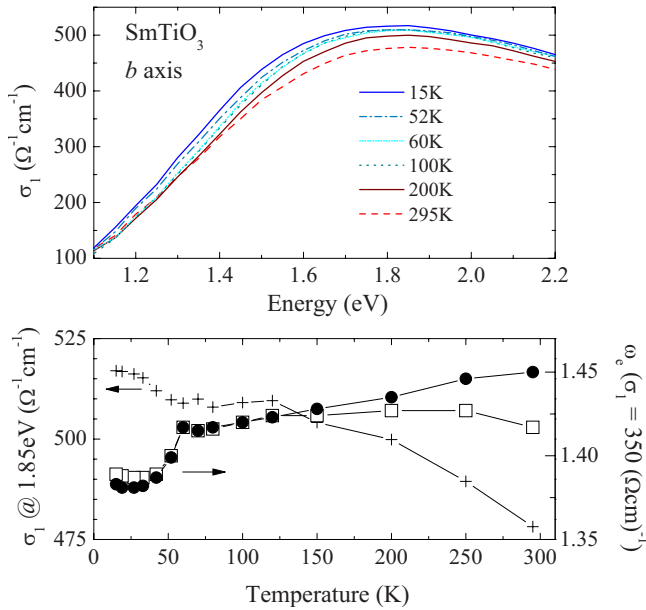


FIG. 6. (Color online) Top: Leading edge of the optical conductivity $\sigma_1^b(\omega)$ of SmTiO_3 . Bottom: Temperature dependence of $\sigma_1^b(\omega=1.85 \text{ eV})$ (crosses, left axis) and of the leading edge ω_e , which we define by $\sigma_1^b(\omega_e)=350(\Omega \text{ cm})^{-1}$ (full symbols, right axis). Open symbols show $\tilde{\omega}_e$ corrected for the change of the spectral weight, i.e., $\sigma_1^b(\tilde{\omega}_e)=c \cdot 350(\Omega \text{ cm})^{-1}$ with $c=\sigma_1^b(1.85 \text{ eV}, T)/\sigma_1^b(1.85 \text{ eV}, 60 \text{ K})$.

that the shift of ω_e is not due to the change of the spectral weight, but is caused mainly by a softening of the peak frequency or a change in the line-shape. Both can be rationalized if the kinetic energy contributes to the attractive interactions responsible for exciton formation. As discussed for 2D compounds in the introduction, the kinetic part results from the different bandwidths or kinetic energies of single particles (order of J in an antiferromagnet) compared to excitons (order of t). This is expected to depend on the spin-spin correlations and therefore also on temperature. The spin-spin correlations and therefore also the attractive interactions are enhanced in the AF ordered state, pulling the spectral weight to lower frequencies with decreasing temperature, in particular in the vicinity of T_N . Remarkably, the peak frequency of 1.95 eV is independent of temperature in the ferromagnet YTiO_3 . It is an interesting question whether this difference between the two compounds arises from the change of the magnetic ground state and reflects the contribution of the kinetic energy to the attractive interactions in antiferromagnetic SmTiO_3 . A decisive identification of the driving force for exciton formation requires further theoretical investigations of the extended multiorbital Hubbard model in 3D.

The peak at 3.7 eV coincides with the minimum of $\sigma_1(\omega)$ observed in YTiO_3 . This peak can be attributed to the lowest singlet multiplet (1T_2 and 1E in cubic symmetry). Due to the spin selection rule, the excitation to the singlet state is suppressed in ferromagnetic YTiO_3 , but it is allowed in antiferromagnetic SmTiO_3 . This feature is expected at about $2J_H \approx 1.2\text{--}1.3 \text{ eV}$ above the lowest triplet peak, providing further support for the assignment of peak B at 2.5 eV and the

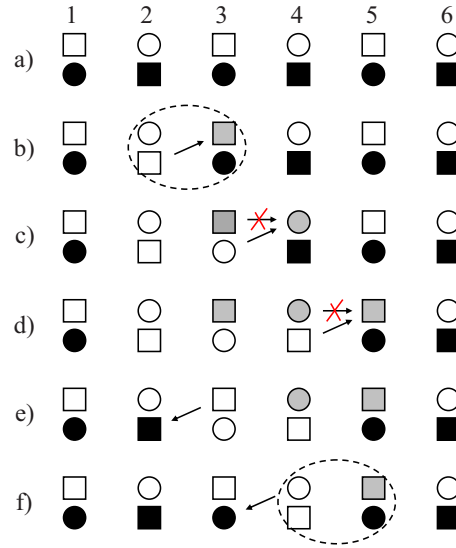


FIG. 7. (Color online) Sketch of the suggested formation and propagation of a Hubbard exciton (dashed line). We consider two types of orbitals (circles and squares, e.g., d_{xy} and d_{xz}) per site, where hopping is zero between orbitals of different type (crossed out arrows). Full (open) symbols denote occupied (empty) orbitals. (a) Ground state with antiferro-orbital order. (b) Creation of a hole and a double occupancy on sites 2 and 3, respectively. (c)–(f) Propagation of the double occupancy, the hole, or of an exciton (see main text for more details).

excitonic character of the peaks at 1.8 eV in SmTiO_3 and 1.95 eV in YTiO_3 .

B. Hubbard exciton and orbital order

For a 2D Mott-Hubbard insulator with AF exchange J on a square lattice, exciton formation is governed by the *kinetic* energy.^{18–22} The motion of a single particle is hindered by the interaction of its spin with the AF background. This can be described in terms of a spin polaron. Hopping of the bare particle on the energy scale t results in a trace of misaligned spins. Coherent motion of the dressed polaronic quasiparticle requires the emission of magnons, i.e., the bare bandwidth $\sim t$ is reduced to the polaronic bandwidth $\sim J$, which corresponds to an increase of kinetic energy. In this case, the kinetic energy is lowered by the formation of *spinless* excitons, which recover a larger bandwidth.

This mechanism may contribute to exciton binding in antiferromagnetic SmTiO_3 , but not in ferromagnetic YTiO_3 . It is promising to investigate whether a similar mechanism is at work in the case of antiferro-*orbital* order. For illustration and simplicity, we consider a 1D model with two orbitals per site, e.g., d_{xy} and d_{xz} for a chain running along the x direction. In Fig. 7, the two types of orbitals are denoted by circles and squares, respectively. Hopping between neighboring sites is allowed only between orbitals of the same type; it is zero between orbitals of different type. Black and gray symbols in Fig. 7 refer to occupied orbitals, whereas empty symbols denote empty orbitals. The ground state in Fig. 7(a) exhibits antiferro-orbital order, i.e., xy (circles) and xz orbitals (squares) are occupied in an alternate fashion. The empty

orbitals are at higher energies due to, e.g., the ligand-field splitting. An excitation from the LHB to the UHB, i.e., $|d^1 d^1\rangle \rightarrow |d^0 d^2\rangle$, is illustrated in Fig. 7(b). Site 2 is empty and site 3 is doubly occupied. The motion of the double occupancy to sites 4 and 5 is depicted in Figs. 7(c) and 7(d), respectively. The central point is that this motion leaves a trace of orbitally excited states, i.e., on sites 3 and 4 the energetically unfavorable orbitals are occupied (gray symbols). This results from the restriction that hopping is only allowed within the same type of orbital. As discussed above for the case of spins, coherent motion of the quasiparticle requires the emission of orbital excitations, in our example the de-excitation of sites 3 and 4. Therefore, the bandwidth is reduced from the bare bandwidth $\sim t$ to the energy scale of the orbital excitations, corresponding to an increase of kinetic energy. However, if the hole accompanies the double occupancy forming an exciton (dashed line), the motion of the hole heals out the trace of excited orbitals [see Figs. 7(e) and 7(f)]. Therefore, the motion of the exciton is not hindered by the antiferro-orbital order, and the exciton can hop on a larger energy scale than the hole or the double occupancy individually. Thus exciton formation here is equivalent to a gain of kinetic energy.

More detailed knowledge on the value of the nearest-neighbor Coulomb interaction V and its relationship to the binding energy in 3D Mott-Hubbard insulators is required to decide whether this mechanism is realized in YTiO_3 . The orbital ordering pattern in YTiO_3 is more complex than simple antiferro-orbital order,^{32,33} and hopping between orbitals of different type is not exactly zero. Still Fig. 7 may be relevant for the ab plane, since hopping from the lowest orbital on one site (a “circle” in Fig. 7) to the lowest orbital on a neighboring site (equivalent to a “square”) is two to three times smaller than hopping to the excited states.^{60,63}

C. Temperature dependence of the spectral weight: spin and orbital selection rules

The spectral weight is determined by the spin and orbital selection rules.^{4,35–46} Therefore, the T dependence of the spectral weight is expected to reflect changes of the spin-spin correlations and/or of the orbital occupation. By considering the nearest-neighbor spin-spin correlations, the absolute value of the spectral weight has been calculated for instance for LaMnO_3 ^{4,35,36} and LaSrMnO_4 .³⁸ These calculations yield a convincing description of the experimental results; the maximum difference is less than a factor of 2. For a 3D magnet one expects that the spin-spin correlations are small above the ordering temperature. In fact, the change of the spectral weight above T_N is small in the 3D antiferromagnet LaMnO_3 .³⁵ In contrast, the 2D antiferromagnet LaSrMnO_4 with a Néel temperature of $T_N=130$ K exhibits a significant T dependence of the spectral weight up to 300 K, which can be attributed to enhanced quantum fluctuations in 2D.³⁸

For the lowest excited triplet state (3T_1 in cubic notation) of orbitally ordered YTiO_3 , Oles *et al.*³⁶ predicted a change of 25% of the spectral weight between the paramagnetic and the ferromagnetic state in the ab and c directions. This can be understood by the evolution of the nearest-neighbor spin-

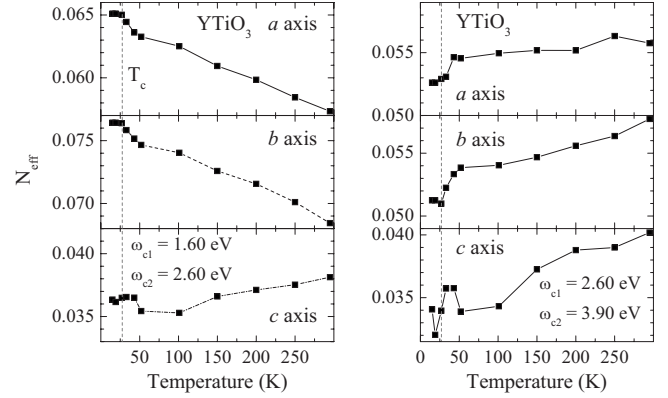


FIG. 8. Temperature dependence of the effective carrier concentration N_{eff} [see Eq. (1)] of YTiO_3 for $\omega_{c1}=1.6$ eV and $\omega_{c2}=2.6$ eV (left) and for $\omega_{c1}=2.6$ eV and $\omega_{c2}=3.9$ eV (right).

spin correlation function $\langle \mathbf{S}_i \cdot \mathbf{S}_j + 3/4 \rangle$, which equals 1 in the ferromagnetic state and $3/4$ in the paramagnetic state, i.e., a redistribution of 25%.

We analyze the integrated spectral weight in terms of the effective carrier concentration N_{eff} ,

$$N_{\text{eff}} = \frac{2mV_0}{\pi e^2} \int_{\omega_{c1}}^{\omega_{c2}} \sigma_1(\omega) d\omega, \quad (1)$$

where ω_{c1} and ω_{c2} denote the frequency range of interest, m is the free electron mass, e the elementary charge, and $1/V_0$ the density of Ti ions. For V_0 we use the value observed at 290 K, which differs from the 2 K value by less than 1%.³⁴ The T dependence of N_{eff} is given in Fig. 8 for YTiO_3 and in Fig. 9 for SmTiO_3 . In YTiO_3 , the spectral weight increases between 1.6 and 2.6 eV (left panel of Fig. 8) in the a and b directions upon cooling down from room temperature. We find an anomaly in the vicinity of T_c , i.e., an additional increase of spectral weight with decreasing temperature. This additional increase starts at about $1.5\text{--}2 T_c$ and amounts to less than 5% below 50 K, much smaller than predicted. At the same time, one finds an anomalous decrease of spectral weight with decreasing temperature between 2.6 and 3.9 eV,

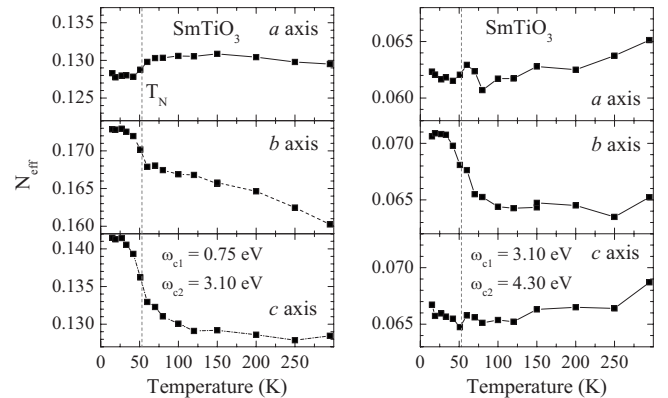


FIG. 9. Temperature dependence of the effective carrier concentration N_{eff} [see Eq. (1)] of SmTiO_3 for $\omega_{c1}=0.75$ eV and $\omega_{c2}=3.1$ eV (left) and for $\omega_{c1}=3.1$ eV and $\omega_{c2}=4.3$ eV (right).

again in a and b . Moreover, the spin selection rule cannot explain that the spectral weight in this 3D ferromagnet shows a strong T dependence up to $300\text{ K} > 10T_c$.

In SmTiO_3 , we also find pronounced anomalies in the vicinity of the magnetic ordering temperature, $T_N=53\text{ K}$. The strongest change of N_{eff} of up to 10% is observed in the c axis, significantly larger than in YTiO_3 . In SmTiO_3 , the *sign* of the change at T_N depends on the polarization (see left panel of Fig. 9), which certainly cannot be attributed to the spin selection rule in a G -type antiferromagnet. In comparison to the excellent agreement found between experiment and theory in the manganites,^{35,38} this failure appears as a puzzle.

Alternatively, we consider the orbital selection rule. In the manganites, the orbital occupation has been assumed to be independent of T due to the large e_g splitting of roughly 1 eV.^{35,38} In both YTiO_3 and SmTiO_3 , the t_{2g} splitting is only $\approx 0.25\text{ eV}$,^{51,59,61} opening the possibility for small changes of the orbital occupation as a function of T . A change of the orbital occupation affects the effective Ti-Ti hopping amplitude t , with $N_{\text{eff}} \propto t^2 \propto t_{pd}^4 / \Delta^2$. An increase of the occupation of the planar xy orbital may for instance give rise to an increase of the spectral weight within the xy plane accompanied by a decrease of spectral weight along z . Thus a change of the orbital occupation at T_N can very well account for the observed polarization dependence. Based on a detailed analysis of the crystal structure, thermal expansion and magnetostriction of RTiO_3 , Komarek *et al.*³⁴ conclude that magnetism affects the crystal structure, which in turn drives a change of the orbital occupation. Remarkably, the shape of the oxygen octahedra changes significantly as a function of temperature, whereas the variation of the tilt and rotation angles is small.³⁴ Both the lattice distortions and the orbital occupation adapt in order to enhance the gain of energy within the spin system. The effect is most pronounced at the magnetic ordering temperature, but extends also to higher temperatures, in agreement with our data. Moreover, Komarek *et al.*³⁴ pointed out that the change of the orbital occupation is significantly stronger in SmTiO_3 than in YTiO_3 , again in agreement with our results. The occurrence of pronounced effects in SmTiO_3 is attributed to the fact that SmTiO_3 is close to the crossover from antiferromagnetic to ferromagnetic order.³⁴ In the optical data, the effect of the orbital selection rule possibly overrules that of the spin selection rule, which appears as a failure of the latter.

Note that the change of the lattice constants at T_N can only account for a change of N_{eff} on the order of 1%. This estimate is based on the Harrison rules⁷⁰ for the hopping amplitudes. We emphasize that binding phenomena such as the formation of excitons or resonances in general are very sensitive to temperature. With decreasing temperature, the attractive interactions responsible for the exciton formation pull down the spectral weight to lower energies, in agreement with the change of the line shape observed in YTiO_3 (see Fig. 3) and the shift of the absorption edge of SmTiO_3 (reflecting a temperature dependence of the attractive interactions; see discussion of Fig. 6 above).

D. Anisotropy

In order to understand the anisotropy observed in YTiO_3 between the ab plane and the c direction, we address the

matrix elements for the optical excitation $|d^1 d^1\rangle \rightarrow |d^0 d^2\rangle$. Our Hamiltonian includes the crystal field, the on-site Coulomb correlations of the d^2 configurations, and the hopping between the two Ti sites (for details, see Ref. 60). We find realistic values of the exchange coupling constants for the different directions as well as an orbital ground state which is in excellent agreement with x-ray, neutron and other theoretical results.^{32,33,51,63,71} From the effective Ti-Ti hopping matrices t^{ab} and t^c one can estimate the anisotropy of the spectral weight from

$$\frac{N_{\text{eff}}^{ab}}{N_{\text{eff}}^c} = \frac{N_{\text{eff}}^a + N_{\text{eff}}^b}{2N_{\text{eff}}^c} = \sum_{j=2,3} \frac{(t_{1j}^{ab})^2 + (t_{j1}^{ab})^2}{(t_{1j}^c)^2 + (t_{j1}^c)^2}, \quad (2)$$

where t_{ij} denotes the effective hopping matrix element between the t_{2g} orbitals i and j on adjacent sites. We obtain $N_{\text{eff}}^{ab}/N_{\text{eff}}^c \approx 5.1$. Using the hopping matrices published by other groups, we find a value of 1.1⁷² or 3.5.⁶³ In the next step the optical conductivity has been calculated using the Kubo formula. We assume a fully polarized ferromagnetic ground state. We address only excitations into the lowest triplet state with a t_{2g}^2 configuration, because here the point-charge approximation gives reliable results. We predict $N_{\text{eff}}^{ab}/N_{\text{eff}}^c \approx 4.5$. The small difference to the value of 5.1 derived from the simplified approach considered in Eq. (2) arises because here the energies of the excited states and the Ti-Ti distance are taken into account. For $\omega_{c1}=1.6\text{ eV}$ and $\omega_{c2}=2.6\text{ eV}$ [see Eq. (1)], we experimentally find $N_{\text{eff}}^{ab}/N_{\text{eff}}^c \approx 2$ (see Fig. 8), within the range predicted by the different theoretical approaches.

IV. SUMMARY AND CONCLUSIONS

In summary, we report on optical excitations from the lower to the upper Hubbard band in the ferromagnet YTiO_3 and in the antiferromagnet SmTiO_3 . At 15 K we find peaks in the optical conductivity $\sigma_1(\omega)$ at 1.95, 2.55, and 4.15 eV in YTiO_3 and at 1.8 and 3.7 eV in SmTiO_3 , which also exhibits a shallow shoulder at 2.5 eV. For these Mott-Hubbard insulators, a local multiplet scenario is expected to yield a reasonable peak assignment, as reported for the manganites.^{35,38} For $U \approx 4.5\text{ eV}$ and $J_H = 0.6 \pm 0.1\text{ eV}$, our local multiplet calculation offers a quantitative description of the peak positions at 2.5, 3.7, and 4.15 eV. The peak at about 2.5 eV is attributed to excitations into the lowest d^2 multiplet (3T_1 in cubic symmetry) with an energy of roughly $U - 3J_H$.⁶² The peak at 3.7 eV corresponds to the lowest d^2 singlet states, and the peak at 4.15 eV is attributed to the lowest state with a $t_{2g}^1 e_g^1$ configuration. This assignment is in agreement with photoemission and LDA+DMFT results. The peaks at 1.95 eV in YTiO_3 and 1.8 eV in SmTiO_3 are interpreted in terms of an excitonic resonance, thereby explaining their low energy.

The temperature dependence of the spectral weight disagrees with predictions based on the spin selection rule. In YTiO_3 the observed temperature dependence is much smaller than predicted, whereas in SmTiO_3 even the sign of the temperature dependence disagrees for certain polarization directions, which is a puzzling result. However, a small

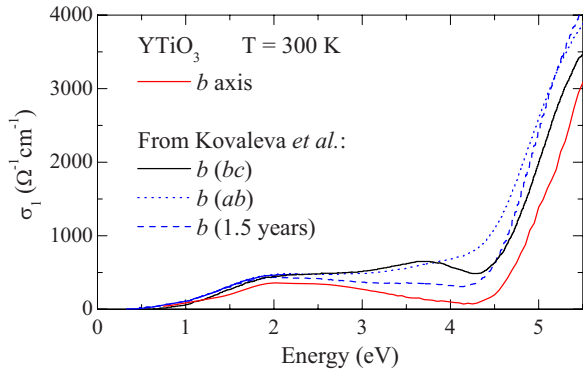


FIG. 10. (Color online) Comparison of the optical conductivity for the b axis of YTiO_3 with spectra reported by Kovaleva *et al.* (Ref. 52), which were determined from either the ab or the bc surface of a freshly polished sample, or from the ab surface of a sample measured after 1.5 years.

change of the orbital occupation at the magnetic ordering temperature³⁴ can account for the polarization dependence and also explains the larger temperature dependence found for SmTiO_3 . In contrast to the manganites, such a change of the orbital occupation is feasible in RTiO_3 because the t_{2g} splitting amounts to only 0.25 eV. Furthermore, the increase of spectral weight at low frequencies with decreasing temperature is in agreement with an exciton scenario, since binding phenomena are expected to exhibit a strong temperature dependence. Moreover, the anomalous softening of the leading absorption edge observed in SmTiO_3 can be explained by the temperature dependence of the contribution of the kinetic energy to the attractive interactions responsible for exciton formation.

The importance of excitonic effects for the description of $\sigma(\omega)$ is well established for low-dimensional correlated insulators. The attractive interaction responsible for exciton formation arises from a gain of either Coulomb or kinetic energy. We have pointed out that exciton formation may lower the kinetic energy in an orbitally ordered state. Our results call for further theoretical studies of exciton formation in the extended multiorbital Hubbard model in 3D. A quantitative description of this binding phenomenon is essential for a consistent explanation of optical and photoemission data and will provide important information on electronic correlations in Hubbard systems.

ACKNOWLEDGMENTS

We thank I. Simons and M. Cwik for technical support, and T. Wagner, D. I. Khomskii, G. S. Uhrig, E. Pavarini, O. K. Andersen, N. Blümer, G. Khaliullin, T. Möller, and S. V. Streltsov for fruitful discussions. This work was supported by the DFG via SFB 608.

APPENDIX: ROLE OF OXYGEN DEFECTS

Recently, Kovaleva *et al.*⁵² studied YTiO_3 by ellipsometry and reported on complications which they attribute to oxygen defects arising from polar surfaces. They observed peaks in $\sigma_1(\omega)$ at 1.95, 2.9, and 3.7 eV. The overall temperature dependence observed in Ref. 52 is very weak, showing a crossover at 100 K, but no anomaly at T_c within the experimental accuracy. In the frequency range studied by us, the main effects of oxygen defects were identified as (i) a shift of the fundamental absorption edge to lower frequencies, (ii) an absorption band at about 0.8 eV, (iii) the absence of a pronounced minimum at 4.5 eV, and (iv) a shift of the onset of charge-transfer excitations to lower frequencies. These shifts have been attributed to localized states at the edge of the electronic bands. This sensitivity of the fundamental absorption edge to doping away from the half-filled Mott insulator has been studied in $\text{Y}_{1-x}\text{Ca}_x\text{TiO}_3$.^{73,74} In Fig. 10 we compare our data with the results of Ref. 52. Our data show both the largest fundamental absorption edge and the largest onset frequency for charge-transfer excitations, in combination with a pronounced minimum at 4.5 eV. We find good agreement with the spectrum of $\sigma_1(\omega)$ below the fundamental gap determined in our group by transmittance and reflectance measurements on thin single crystals⁵¹ (see Fig. 2). The transmittance clearly reveals bulk properties. These data show no defect-induced absorption below the gap; the single weak feature observed at about 0.3 eV has been undoubtedly identified as a phonon-activated orbital excitation.^{51,59,61} Finally, we find clear anomalies in the vicinity of the magnetic ordering temperatures, both in YTiO_3 and in SmTiO_3 (see Figs. 8 and 9). The combination of all these observations provides strong evidence that we have observed the intrinsic properties of YTiO_3 .

¹G. Kotliar and D. Vollhardt, *Phys. Today* **57**(3), 53 (2004).

²M. Imada, A. Fujimori, and Y. Tokura, *Rev. Mod. Phys.* **70**, 1039 (1998).

³Y. Tokura and N. Nagaosa, *Science* **288**, 462 (2000).

⁴G. Khaliullin, *Prog. Theor. Phys. Suppl.* **160**, 155 (2005).

⁵D. I. Khomskii, *Phys. Scr.* **72**, CC8 (2005).

⁶J. van den Brink, M. B. J. Meinders, J. Lorenzana, R. Eder, and G. A. Sawatzky, *Phys. Rev. Lett.* **75**, 4658 (1995).

⁷F. B. Gallagher and S. Mazumdar, *Phys. Rev. B* **56**, 15025 (1997).

⁸R. Neudert, M. Knupfer, M. S. Golden, J. Fink, W. Stephan, K.

Penc, N. Motoyama, H. Eisaki, and S. Uchida, *Phys. Rev. Lett.* **81**, 657 (1998).

⁹F. H. L. Essler, F. Gebhard, and E. Jeckelmann, *Phys. Rev. B* **64**, 125119 (2001).

¹⁰A. Hübsch, J. Richter, C. Waidacher, K. W. Becker, and W. von der Linden, *Phys. Rev. B* **63**, 205103 (2001).

¹¹E. Jeckelmann, *Phys. Rev. B* **67**, 075106 (2003).

¹²A. S. Moskvina, J. Málek, M. Knupfer, R. Neudert, J. Fink, R. Hayn, S. L. Drechsler, N. Motoyama, H. Eisaki, and S. Uchida, *Phys. Rev. Lett.* **91**, 037001 (2003).

¹³Y.-J. Kim, J. P. Hill, H. Benthien, F. H. L. Essler, E. Jeckelmann,

- H. S. Choi, T. W. Noh, N. Motoyama, K. M. Kojima, S. Uchida, D. Casa, and T. Gog, *Phys. Rev. Lett.* **92**, 137402 (2004).
- ¹⁴H. Matsueda, T. Tohyama, and S. Maekawa, *Phys. Rev. B* **71**, 153106 (2005).
- ¹⁵M. Ono, K. Miura, A. Maeda, H. Matsuzaki, H. Kishida, Y. Taguchi, Y. Tokura, M. Yamashita, and H. Okamoto, *Phys. Rev. B* **70**, 085101 (2004).
- ¹⁶M. Ono, H. Kishida, and H. Okamoto, *Phys. Rev. Lett.* **95**, 087401 (2005).
- ¹⁷H. Kishida, H. Matsuzaki, H. Okamoto, T. Manabe, M. Yamashita, Y. Taguchi, and Y. Tokura, *Nature (London)* **405**, 929 (2000).
- ¹⁸D. G. Clarke, *Phys. Rev. B* **48**, 7520 (1993).
- ¹⁹Y. Y. Wang, F. C. Zhang, V. P. Dravid, K. K. Ng, M. V. Klein, S. E. Schnatterly, and L. L. Miller, *Phys. Rev. Lett.* **77**, 1809 (1996).
- ²⁰F. C. Zhang and K. K. Ng, *Phys. Rev. B* **58**, 13520 (1998).
- ²¹P. Wrobel and R. Eder, *Phys. Rev. B* **66**, 035111 (2002).
- ²²R. O. Kuzian, R. Hayn, and A. F. Barabanov, *Phys. Rev. B* **68**, 195106 (2003).
- ²³M. E. Símón, A. A. Aligia, C. D. Batista, E. R. Gagliano, and F. Lema, *Phys. Rev. B* **54**, R3780 (1996).
- ²⁴E. Hanamura, N. T. Dan, and Y. Tanabe, *Phys. Rev. B* **62**, 7033 (2000); *J. Phys.: Condens. Matter* **12**, L345 (2000).
- ²⁵A. S. Moskvin, R. Neudert, M. Knupfer, J. Fink, and R. Hayn, *Phys. Rev. B* **65**, 180512(R) (2002).
- ²⁶H. Gomi, A. Takahashi, T. Ueda, H. Itoh, and M. Aihara, *Phys. Rev. B* **71**, 045129 (2005).
- ²⁷H. Itoh, A. Takahashi, and M. Aihara, *Phys. Rev. B* **73**, 075110 (2006).
- ²⁸E. Collart, A. Shukla, J.-P. Rueff, P. Leininger, H. Ishii, I. Jarriège, Y. Q. Cai, S.-W. Cheong, and G. Dhalenne, *Phys. Rev. Lett.* **96**, 157004 (2006).
- ²⁹D. S. Ellis, J. P. Hill, S. Wakimoto, R. J. Birgeneau, D. Casa, T. Gog, and Y.-J. Kim, *Phys. Rev. B* **77**, 060501(R) (2008).
- ³⁰J. E. Hirsch, *Phys. Rev. Lett.* **59**, 228 (1987); *Science* **295**, 2226 (2002).
- ³¹H. J. A. Molegraaf, C. Presura, D. van der Marel, P. H. Kes, and M. Li, *Science* **295**, 2239 (2002).
- ³²J. Akimitsu, H. Ichikawa, N. Eguchi, T. Miyano, M. Nishi, and K. Kakurai, *J. Phys. Soc. Jpn.* **70**, 3475 (2001).
- ³³F. Iga, M. Tsubota, M. Sawada, H. B. Huang, S. Kura, M. Take-mura, K. Yaji, M. Nagira, A. Kimura, T. Jo, T. Takabatake, H. Namatame, and M. Taniguchi, *Phys. Rev. Lett.* **93**, 257207 (2004).
- ³⁴A. C. Komarek, H. Roth, M. Cwik, W.-D. Stein, J. Baier, M. Kriener, F. Bourée, T. Lorenz, and M. Braden, *Phys. Rev. B* **75**, 224402 (2007).
- ³⁵N. N. Kovaleva, A. V. Boris, C. Bernhard, A. Kulakov, A. Pimenov, A. M. Balbashov, G. Khaliullin, and B. Keimer, *Phys. Rev. Lett.* **93**, 147204 (2004).
- ³⁶A. M. Oles, G. Khaliullin, P. Horsch, and L. F. Feiner, *Phys. Rev. B* **72**, 214431 (2005).
- ³⁷J. S. Lee, M. W. Kim, and T. W. Noh, *New J. Phys.* **7**, 147 (2005).
- ³⁸A. Gössling, M. W. Haverkort, M. Benomar, Hua Wu, D. Senff, T. Möller, M. Braden, J. A. Mydosh, and M. Grüninger, *Phys. Rev. B* **77**, 035109 (2008).
- ³⁹K. H. Ahn and A. J. Millis, *Phys. Rev. B* **61**, 13545 (2000).
- ⁴⁰K. Tobe, T. Kimura, Y. Okimoto, and Y. Tokura, *Phys. Rev. B* **64**, 184421 (2001).
- ⁴¹J. S. Lee, Y. S. Lee, T. W. Noh, S.-J. Oh, J. Yu, S. Nakatsuji, H. Fukazawa, and Y. Maeno, *Phys. Rev. Lett.* **89**, 257402 (2002).
- ⁴²M. W. Kim, Y. S. Lee, T. W. Noh, J. Yu, and Y. Moritomo, *Phys. Rev. Lett.* **92**, 027202 (2004).
- ⁴³R. Rauer, M. Rübhausen, and K. Dörr, *Phys. Rev. B* **73**, 092402 (2006).
- ⁴⁴S. Miyasaka, Y. Okimoto, and Y. Tokura, *J. Phys. Soc. Jpn.* **71**, 2086 (2002).
- ⁴⁵A. A. Tsvetkov, F. P. Mena, P. H. M. van Loosdrecht, D. van der Marel, Y. Ren, A. A. Nugroho, A. A. Menovsky, I. S. Elfimov, and G. A. Sawatzky, *Phys. Rev. B* **69**, 075110 (2004).
- ⁴⁶G. Khaliullin, P. Horsch, and A. M. Oleś, *Phys. Rev. B* **70**, 195103 (2004).
- ⁴⁷H. Roth, Ph.D. thesis, University of Cologne, 2008.
- ⁴⁸M. Schubert, *Phys. Rev. B* **53**, 4265 (1996).
- ⁴⁹A. Gössling, Ph.D. thesis, University of Cologne, 2007; <http://nbn-resolving.de/urn:nbn:de:hbz:38-21379>
- ⁵⁰T. Arima, Y. Tokura, and J. B. Torrance, *Phys. Rev. B* **48**, 17006 (1993).
- ⁵¹R. Rückamp, E. Benckiser, M. W. Haverkort, H. Roth, T. Lorenz, A. Freimuth, L. Jongen, A. Möller, G. Meyer, P. Reutler, B. Büchner, A. Revcolevschi, S.-W. Cheong, C. Sekar, G. Krabbes, and M. Grüninger, *New J. Phys.* **7**, 144 (2005).
- ⁵²N. N. Kovaleva, A. V. Boris, P. Yordanov, A. Maljuk, E. Brücher, J. Stremper, M. Konuma, I. Zegkinoglou, C. Bernhard, A. M. Stoneham, and B. Keimer, *Phys. Rev. B* **76**, 155125 (2007).
- ⁵³A. Fujimori, I. Hase, H. Namatame, Y. Fujishima, Y. Tokura, H. Eisaki, S. Uchida, K. Takegahara, and F. M. F. de Groot, *Phys. Rev. Lett.* **69**, 1796 (1992).
- ⁵⁴A. E. Bocquet, T. Mizokawa, K. Morikawa, A. Fujimori, S. R. Barman, K. Maiti, D. D. Sarma, Y. Tokura, and M. Onoda, *Phys. Rev. B* **53**, 1161 (1996).
- ⁵⁵K. Morikawa, T. Mizokawa, A. Fujimori, Y. Taguchi, and Y. Tokura, *Phys. Rev. B* **54**, 8446 (1996).
- ⁵⁶For a comparison of different results one needs to distinguish between $U = F^0 + \frac{4}{49}F^2 + \frac{36}{441}F^4$ (both electrons occupy the *same* real orbital) and $U_{av} = F^0 - \frac{14}{441}(F^2 + F^4)$ (averaged over all multiplets) with the Slater integrals F^0 , F^2 , and F^4 . The value of $U_{av} \cong 4$ eV reported in Ref. 54 corresponds to $U \approx 5.3$ eV. However, this value is based on a TiO_6 configuration-interaction cluster model including covalency. Due to screening effects by O_{2p} orbitals, the effective value of U is somewhat smaller, in good agreement with $U = 4.5$ eV chosen in Fig. 5.
- ⁵⁷S. Sugano, Y. Tanabe, and H. Kamimura, *Multiplets of Transition-Metal Ions in Crystals* (Academic, New York, 1970).
- ⁵⁸T. Higuchi, T. Tsukamoto, M. Watanabe, M. M. Grush, T. A. Callcott, R. C. Perera, D. L. Ederer, Y. Tokura, Y. Harada, Y. Tezuka, and S. Shin, *Phys. Rev. B* **60**, 7711 (1999).
- ⁵⁹C. Ulrich, G. Ghiringhelli, A. Piazzalunga, L. Braicovich, N. B. Brookes, H. Roth, T. Lorenz, and B. Keimer, *Phys. Rev. B* **77**, 113102 (2008).
- ⁶⁰R. Schmitz, O. Entin-Wohlman, A. Aharony, and E. Müller-Hartmann, *Ann. Phys.* **16**, 425 (2007); **14**, 626 (2005).
- ⁶¹C. Ulrich, A. Gössling, M. Grüninger, M. Guennou, H. Roth, M. Cwik, T. Lorenz, G. Khaliullin, and B. Keimer, *Phys. Rev. Lett.* **97**, 157401 (2006).
- ⁶²The t_{2g} splitting $\Delta_{t_{2g}}$ is relevant for a precise determination of U , since the lowest nonexcitonic excitation (peak B) is expected at about $U - 3J_H + \Delta_{t_{2g}}$.

- ⁶³E. Pavarini, A. Yamasaki, J. Nuss, and O. K. Andersen, *New J. Phys.* **7**, 188 (2005).
- ⁶⁴L. Craco, S. Leoni, M. S. Laad, and H. Rosner, *Phys. Rev. B* **76**, 115128 (2007).
- ⁶⁵M. Arita, H. Sato, M. Higashi, K. Yoshikawa, K. Shimada, M. Nakatake, Y. Ueda, H. Namatame, M. Taniguchi, M. Tsubota, F. Iga, and T. Takabatake, *Phys. Rev. B* **75**, 205124 (2007).
- ⁶⁶In Mott-Hubbard insulators, the particle and the hole may reside on the *same* site, albeit with different spin or orbital quantum numbers. Such a very strongly bound “exciton” corresponds to a magnon or an orbiton, excitations within the spin or orbital channel. There is no doubly occupied site and one does not have to pay the energy U , in contrast to the excitations discussed here.
- ⁶⁷M. Mochizuki and M. Imada, *New J. Phys.* **6**, 154 (2004).
- ⁶⁸M. Mochizuki and M. Imada, *J. Phys. Soc. Jpn.* **73**, 1833 (2004).
- ⁶⁹M. Kubota, H. Nakao, Y. Murakami, Y. Taguchi, M. Iwama, and Y. Tokura, *Phys. Rev. B* **70**, 245125 (2004).
- ⁷⁰W. A. Harrison, *Elementary Electronic Structure* (World Scientific, Singapore, 1999).
- ⁷¹S. V. Streltsov, A. S. Mylnikova, A. O. Shorikov, Z. V. Pchelkina, D. I. Khomskii, and V. I. Anisimov, *Phys. Rev. B* **71**, 245114 (2005).
- ⁷²I. V. Solovyev, *Phys. Rev. B* **73**, 155117 (2006).
- ⁷³Y. Okimoto, T. Katsufuji, Y. Okada, T. Arima, and Y. Tokura, *Phys. Rev. B* **51**, 9581 (1995).
- ⁷⁴Y. Taguchi, Y. Tokura, T. Arima, and F. Inaba, *Phys. Rev. B* **48**, 511 (1993).